AFRL-RX-WP-JA-2017-0196

STUDY OF MINORITY CARRIER LIFETIMES IN VERY LONG-WAVE INFRARED STRAINED-LAYER InAs/GaInSb SUPERLATTICES (POSTPRINT)

B. V. Olson, E. A. Kadlec, J. K. Kim, and E. A. Shaner

Sandia National Laboratories

H.J. Haugan and Gail J. Brown

AFRL/RX

18 July 2016
Interim Report

(STINFO COPY)

AIR FORCE RESEARCH LABORATORY
MATERIALS AND MANUFACTURING DIRECTORATE
WRIGHT-PATTERSON AIR FORCE BASE, OH 45433-7750
AIR FORCE MATERIEL COMMAND
UNITED STATES AIR FORCE

REPORT DOCUMENTATION PAGE

Form Approved
OMB No. 0704-0188

1. REPORT DATE *(DD-MM-YY)*	2. REPORT TYPE	3. DATES COVERED *(From - To)*
18 July 2016	Interim	11 September 2013 – 18 Jun 2016

4. TITLE AND SUBTITLE
STUDY OF MINORITY CARRIER LIFETIMES IN VERY LONG-WAVE INFRARED STRAINED-LAYER InAs/GaInSb SUPERLATTICES (POSTPRINT)

5a. CONTRACT NUMBER
FA8650-11-D-5800-0008

5b. GRANT NUMBER

5c. PROGRAM ELEMENT NUMBER
62102F

6. AUTHOR(S)
1) B. V. Olson, E. A. Kadlec, J. K. Kim, and E. A. Shaner - Sandia National Laboratories
2) H.J. Haugan and Gail J. Brown – AFRL/RX

5d. PROJECT NUMBER
4348

5e. TASK NUMBER

5f. WORK UNIT NUMBER
X0TW

7. PERFORMING ORGANIZATION NAME(S) AND ADDRESS(ES)
1) Sandia National Laboratories, 1515 Eubank Blvd SE # 831 Albuquerque, NM 87185
2) AFRL/RX Wright-Patterson AFB, OH 45433

8. PERFORMING ORGANIZATION REPORT NUMBER

9. SPONSORING/MONITORING AGENCY NAME(S) AND ADDRESS(ES)
Air Force Research Laboratory
Materials and Manufacturing Directorate
Wright-Patterson Air Force Base, OH 45433-7750
Air Force Materiel Command
United States Air Force

10. SPONSORING/MONITORING AGENCY ACRONYM(S)
AFRL/RXAN

11. SPONSORING/MONITORING AGENCY REPORT NUMBER(S)
AFRL-RX-WP-JA-2017-0196

12. DISTRIBUTION/AVAILABILITY STATEMENT
Distribution Statement A. Approved for public release: distribution unlimited.

13. SUPPLEMENTARY NOTES
PA Case Number: 88ABW-2016-3512; Clearance Date: 18 July 2016. This document contains color. Journal article published in Proceedings of SPIE, Vol. 9974, 19 Sep 2016. © 2016 SPIE. The U.S. Government is joint author of the work and has the right to use, modify, reproduce, release, perform, display, or disclose the work.
The final publication is available at http://dx.doi.org/10.1117/12.2236535

14. ABSTRACT *(Maximum 200 words)*
Significantly improved carrier lifetimes in very long wavelength infrared (VLWIR) InAs/GaInSb superlattice (SL) absorbers are demonstrated by using time-resolved microwave reflectance (TMR) measurements. A nominal 47.0 Å InAs/21.5 Å Ga0.75In0.25Sb SL structure that produces an approximately 25 μm response at 10 K has a minority carrier lifetime of 140 ± 20 ns at 18 K, which is an order-of-magnitude improvement compare to previously reported lifetime values for other VLWIR detector absorbers. This improvement is attributed to the strain-engineered ternary SL design, which offers a variety of epitaxial advantages and ultimately leads to the improvements in the minority carrier lifetime b mitigating defect-mediated Shockley-Read-Hall (SRH) recombination centers. By analyzing the temperature dependence of TMR decay data, the recombination mechanisms and trap states that currently limit the performance of this SL absorber are identified. The results show a general decrease in the long-decay lifetime component, which is dominated by SRH recombination at temperatures below ~30 K, and by Auger recombination at temperatures above ~45 K.

15. SUBJECT TERMS
Indium arsenide ; Superlattices ; Absorption ; Engineering ; Long wavelength infrared ; Photodetectors ; Reflectivity ; Sensors

16. SECURITY CLASSIFICATION OF:			17. LIMITATION OF ABSTRACT:	18. NUMBER OF PAGES	19a. NAME OF RESPONSIBLE PERSON (Monitor)
a. REPORT	b. ABSTRACT	c. THIS PAGE			Joseph Burns
Unclassified	Unclassified	Unclassified	SAR	12	19b. TELEPHONE NUMBER *(Include Area Code)* (937) 255-9594

Study of minority carrier lifetimes in very long-wave infrared strained-layer InAs/GaInSb superlattices

H. J. Haugan[a], B. V. Olson[b], G. J. Brown[a], E. A. Kadlec[b], J. K. Kim[b], and E. A. Shaner[b]

[a]Air Force Research Laboratory, Materials and Manufacturing Directorate, Wright-Patterson Air Force Base, Ohio 45433
[b]Sandia National Laboratories, Albuquerque, New Mexico 87185

ABSTRACT

Significantly improved carrier lifetimes in very long wavelength infrared (VLWIR) InAs/GaInSb superlattice (SL) absorbers are demonstrated by using time-resolved microwave reflectance (TMR) measurements. A nominal 47.0 Å InAs/21.5 Å $Ga_{0.75}In_{0.25}Sb$ SL structure that produces an approximately 25 μm response at 10 K has a minority carrier lifetime of 140 ± 20 ns at 18 K, which is an order-of-magnitude improvement compare to previously reported lifetime values for other VLWIR detector absorbers. This improvement is attributed to the strain-engineered ternary SL design, which offers a variety of epitaxial advantages and ultimately leads to the improvements in the minority carrier lifetime by mitigating defect-mediated Shockley-Read-Hall (SRH) recombination centers. By analyzing the temperature-dependence of TMR decay data, the recombination mechanisms and trap states that currently limit the performance of this SL absorber are identified. The results show a general decrease in the long-decay lifetime component, which is dominated by SRH recombination at temperatures below ~30 K, and by Auger recombination at temperatures above ~45 K. This result implies that minimal improvement can be made in the minority carrier lifetime at temperatures greater than 45 K without further suppressing Auger recombination through proper band engineering, which suggests that the improvement to be gained by mitigation of the SRH defects would not be substantial at these temperatures. At temperatures lower than 30 K, some improvement can be attained by mitigated of the SRH recombination centers. Since the strain-balanced ternary SL design offers a reasonably good absorption coefficient and many epitaxial advantages during growth, this VLWIR SL material system should be considered a competitive candidate for VLWIR photodetector technology.

1. INTRODUCTION

There is a steady effort in developing infrared (IR) materials that can be used for very long wavelength infrared (VLWIR) detection. Owing to several intrinsic advantages, InAs/GaInSb (noted herein as "ternary") superlattices (SLs) have become an IR material system of focus, particularly for cutoff wavelength range beyond 15 μm [1, 2]. With increasing indium composition, a very narrow bandgap can be achieved with a reasonably small period for this ternary SL system, leading to a larger optical absorption coefficient due to enhanced electron and hole wave function overlaps [3]. More importantly, the strain within the SL layers creates a large splitting between the heavy-hole and light-hole bands in the ternary SLs, reducing the hole-hole Auger recombination process and increasing the best case minority carrier lifetime, thus improving the device detectivity (D*) and operating temperature. Based on minimizing the Auger recombination, Grein *et al*. [4] proposed a strain-balanced VLWIR ternary SL structure of 47.0 Å InAs/21.5 Å $Ga_{0.75}In_{0.25}Sb$. For a hole concentration of 7×10^{16} cm^{-3}, a radiative lifetime of 140 nanoseconds (ns) for this ternary SL was computed, while both the Auger-1 and Auger-7 lifetimes were calculated to be in excess of 1 s. These predictions provide an upper bound device D* of 6.0×10^{14} Jones at 40 K. Despite these Auger recombination advantages, very few research groups have examined VLWIR ternary SL devices to verify these theoretically predicted performance limits. So far, the best reported VLWIR D* is 4.5×10^{10} Jones at 80 K using an InAs/GaSb (noted herein as "binary") SL

Infrared Sensors, Devices, and Applications VI, edited by Paul D. LeVan, Ashok K. Sood, Priyalal Wijewarnasuriya, Arvind I. D'Souza, Proc. of SPIE Vol. 9974, 997403

absorber with a cutoff wavelength of ~19 μm [5]. Short electron lifetimes, in the range of 15-30 ns at 77 K [6-8], are typical for long wavelength infrared (LWIR) binary SL absorbers and these short lifetimes are expected to be even shorter for VLWIR binary SL absorbers by considering the rapid increase in Auger coefficient with increasing cutoff wavelength [9]. Short lifetimes observed in LWIR/VLWIR binary SL absorbers are believed to be originated from Ga-mediated Shockley-Read-Hall (SRH) defects that are generated during the binary SL growth. Longer minority carrier lifetime, up to ~10 μs, have been reported in mid wavelength infrared (MWIR) InAs/InAsSb (noted herein as "Ga-free") SL absorbers [10]. In order to strain balance these Ga-free SLs in a VLWIR design though, a much wider SL period is required. Compared to the ~68 Å used in Grein *et al.*'s [4] calculation, a SL period of 147 Å [11] is required in the Ga-free SL to reach VLWIR bandgaps. This larger SL period significantly impact a photon detector's figures of merit. such as the optical absorption and Auger recombination lifetime. Ternary SLs in general have the advantage of higher absorption, sharper absorption onset, and longer Auger lifetimes relative to the Ga-free SL equivalent. Recently, Haugan *et al*. [12-15] have shown considerable improvements in the optical and electrical quality of VLWIR ternary SL materials by optimizing molecular beam epitaxy (MBE) growth parameters. They implicated that the use of a strain-balanced ternary SL design aided improving the MBE growth process and led to considerable improvements in the optical/electrical quality of VLWIR SL materials. The lower Ga-content, in particular, helped reduce the density of Ga-associated recombination centers and ultimately improved SRH lifetimes [16, 17].

In this report, we compile several lifetime study series [16, 17] previously reported to demonstrate our approach toward improving this new generation of VLWIR detector materials. For our recent growth optimization studies, a nominal SL structure of 47.0 Å InAs/21.5 Å $Ga_{0.75}In_{0.25}Sb$ that was proposed by Grein *et al*. [4] was selected to optimize MBE growth processes. Systematic growth optimization studies were performed in order to maximize the optical response by using 0.5 μm thick SL absorbers [12-15]. After going through various MBE optimization processes, a strong photoresponse (PR) signal with a relatively sharp absorption edge was measured despite the fact that the SL total thickness was only ~3 % of the VLWIR photon wavelength. Since the minority carrier lifetimes of the VLWIR SL absorber ultimately sets the performance upper limits of the D* and detector operating temperature, we use time-resolved microwave reflectance (TMR) measurements to evaluate the recombination quality of optimized 2 μm thick SL absorbers that can be integrated into a photodiode structure at a variety of operating temperatures. The resulting temperature-dependent TMR lifetime data are analyzed using theory for radiative, SRH, and Auger recombination in order to determine the contribution each mechanism has to the observed carrier lifetimes. Identifying the specific recombination mechanisms that are limiting the minority carrier lifetime is critical for designing future VLWIR absorber structure. For instance, the methodology required to improve the carrier lifetime if it is limited by Auger recombination is very different than if it is limited by SRH recombination. While the latter is related to material quality and extrinsic defect states, and can be mitigated by optimizing growth parameters for instance, the former is an intrinsic process that requires engineering the electronic band structure to suppress Auger recombination. The results investigated here will aid the design of long lifetime VLWIR SL absorbers for high quantum efficiency and low dark current IR detectors.

2. EXPERIMENTS

There have been numerous reports on binary SL growth studies [3, 18] exploring the best growth parameters, but very few on ternary SL growth studies. Although general suggestion can be adapted from the binary SL growth to initiate ternary SL optimization process, each growth parameter needs to be adjusted for the growth of a particular ternary SL design of interest. In our case, we used a test structure of 0.5 μm thick 47.0 Å InAs/21.5 Å $Ga_{0.75}In_{0.25}Sb$ SLs to optimize the initial MBE growth parameters for a strong PR signal. For a typical growth optimization experiment, a 0.5 μm thick GaSb buffer layer was grown at ~490 °C and then the ternary SLs at 410-440 °C. The V/III beam flux ratio was set around 3-4 for both GaInSb and InAs layers. The growth rates of 1.6 and 0.3 Å/s were used for GaInSb and InAs layers, respectively. The Sb (As) cracking zone temperature was set at 950 (900) °C. Unlike most VLWIR binary SLs that require an adjusted interface shutter sequence to compensate a large residual SL strain [19, 20], a small residual strain in the ternary SLs was able to be easily compensated without going through complicated interface engineering process to achieve lattice-matched conditions. This is one of significant epitaxial advantages of using the strain-balanced ternary SL design over the binary SL equivalent.

Proc. of SPIE Vol. 9974 997403-2

After going through several growth optimization studies [12-15], the optimum growth condition was established and employed to grow a test structure of thick absorbers that can be incorporated into a diode structure for the lifetime studies. The test structure for lifetime measurements consists of a 2500 Å top $InAs_{0.91}Sb_{0.09}$ cladding layer, a 2 µm thick ternary SL absorber layer, a 2500 Å bottom $InAs_{0.91}Sb_{0.09}$ cladding layer, and a 2500 Å GaSb buffer layer. The nominal ternary SL absorber structure generates approximately 25 micron response at 10 K [12-15]. High-resolution X-ray diffraction (HRXRD) measurements are used to confirm the SL period and residual strain for the samples used for the lifetime studies: 67.1 ± 0.5 Å and 0.01 ± 0.01 %, in reasonably good agreement with intended SL structure (see Fig. 1). This sample has the excellent crystalline quality that can be easily achieved by using the simple growth sequence described in the left insert of Fig. 1.

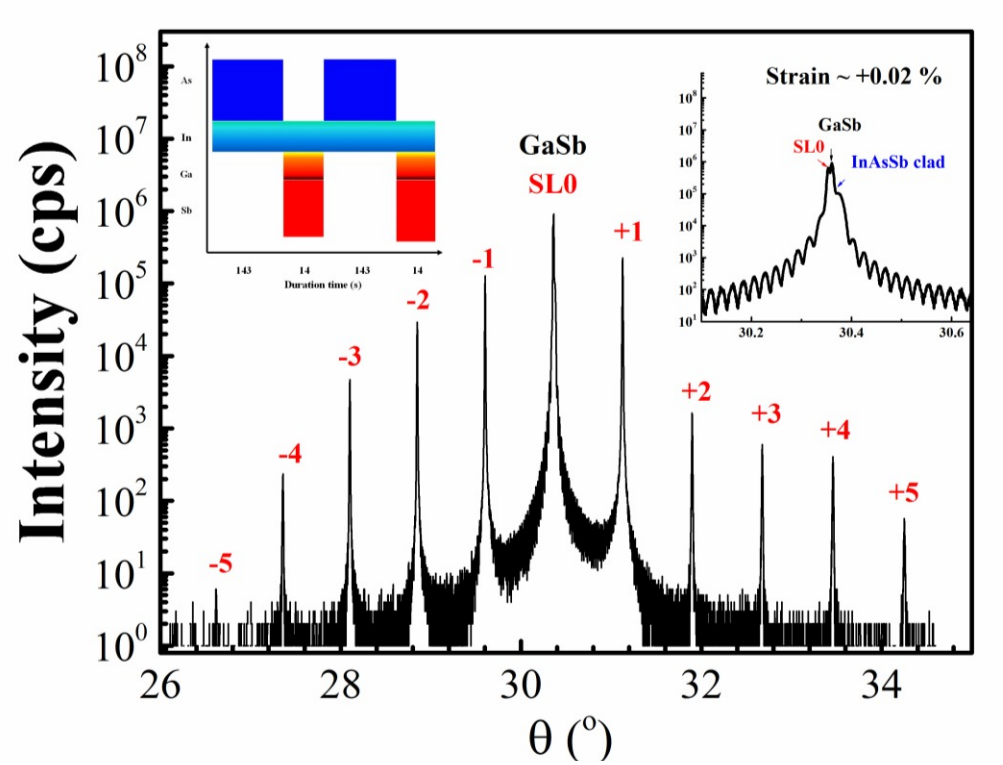

Figure 1. (Color online) X-ray diffraction patterns of a 67.1 ± 0.5 Å period superlattice (SL) sample containing a 2 µm thick 47.0 Å InAs/21.5 Å $Ga_{0.75}In_{0.25}Sb$ SL. The left insert is the shutter sequence employed to create the strain-balanced ternary absorber layer. The right insert is a zoomed view of the center diffraction peak.

A similarly grown 0.5 µm thick ternary SL structure with a measured period of 67.7 ± 0.5 Å produces an approximately 23 µm response (~53 meV) at 10 K, as demonstrated in PR spectrum in Fig. 2. Based on our most recent growth optimization studies [12-15], a majority of optimized VLWIR SL samples produce an overall strong PR signal over a wide wavelength range up to ~15 µm with a relatively sharp band edge, which is important for developing VLWIR photodetectors. Considering reliability of our MBE growth of VLWIR ternary SLs, and a SL period that is similar to characterized diode structures, we estimate that the bandgap of the carrier lifetime sample reported here is approximately 48 ± 5 meV at 10 K.

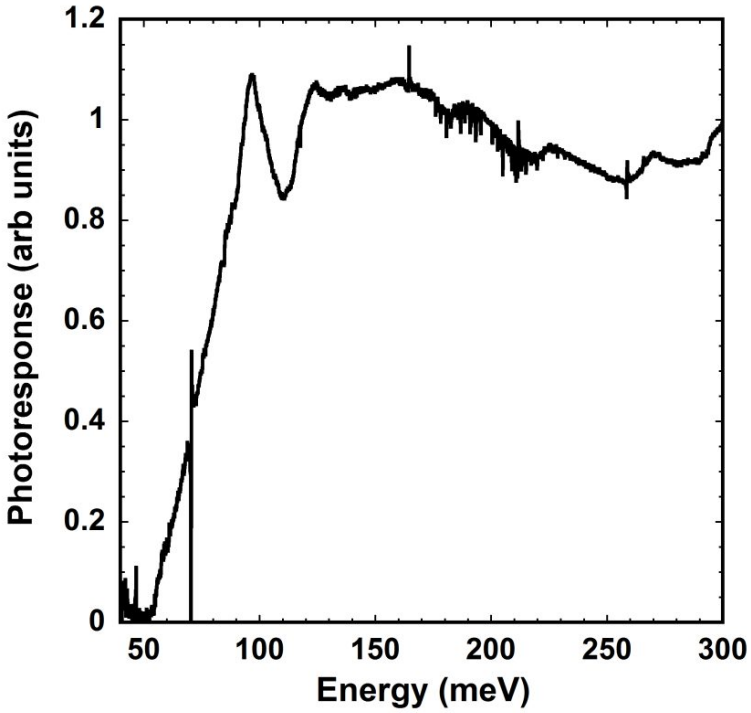

Figure 2. Photoresponse spectrum at 10 K of a 67.7 ± 0.5 Å period ternary superlattice (SL) sample containing a 0.5 µm thick 47.0 Å InAs/21.5 Å $Ga_{0.75}In_{0.75}Sb$ SL absorber. This structure produces an approximately 23 µm response (~53 meV) at 10 K

For lifetime characterization of this ternary SL structure, TMR measurements were performed at a variety of temperatures in order to determine the minority carrier lifetime (τ_{mc}). The TMR technique involves using a pulsed IR laser, in this case a tunable optical parametric oscillator (OPO) set to a wavelength of 5 µm, to optically generate excited charge carriers in the ternary SL absorber region. These excited charge carriers cool rapidly to the SL band edges and alter the conductivity of the sample. Microwaves reflected from the sample surface are sensitive to this change in conductivity. Therefore, by monitoring the reflected microwave signal as a function of time, the decay of the excess carriers, and the carrier lifetime, can be temporally resolved. Additional information on this measurement method can be found elsewhere [21, 22]. The OPO wavelength of 5 µm is used to ensure a nearly uniform distribution of charge is generated throughout the thick SL absorber, eliminating convolutions of the data due to carrier diffusion. This wavelength is also below the bandgap of the GaSb substrate and the $InAs_{0.91}Sb_{0.09}$ cladding layers to ensure that excited charge carriers are only generated in the VLWIR SL absorber region. At this wavelength, the absorption coefficient in the SL (α_{pump}) is approximately 2000 cm^{-1}, calculated using a 14-band $\boldsymbol{k \cdot p}$ code for the ternary SL structure. The initial non-equilibrium excess carrier density is determined using this absorption coefficient and the incident pump fluence. Time-resolved reflectance decays are taken as a function of both pump power (i.e. initial optically generated carrier density) and sample temperature.

3. RESULTS AND DISCUSSIONS

3.1. Recombination qualities

Figure 3a shows TMR decays for a few different initial optically generated carrier densities at a temperature of 18 K. Very rapid decays are observed in the first 50 ns are observed over a wide range of injected carrier densities, which is likely Auger recombination. These rapid initial decays are followed by significantly slower decays at long time scales. To investigate these decays further, the TMR data are converted to instantaneous carrier lifetimes as a function of the excess carrier density (Δn) using previously described analysis methods [21] and are shown in Fig. 3b.

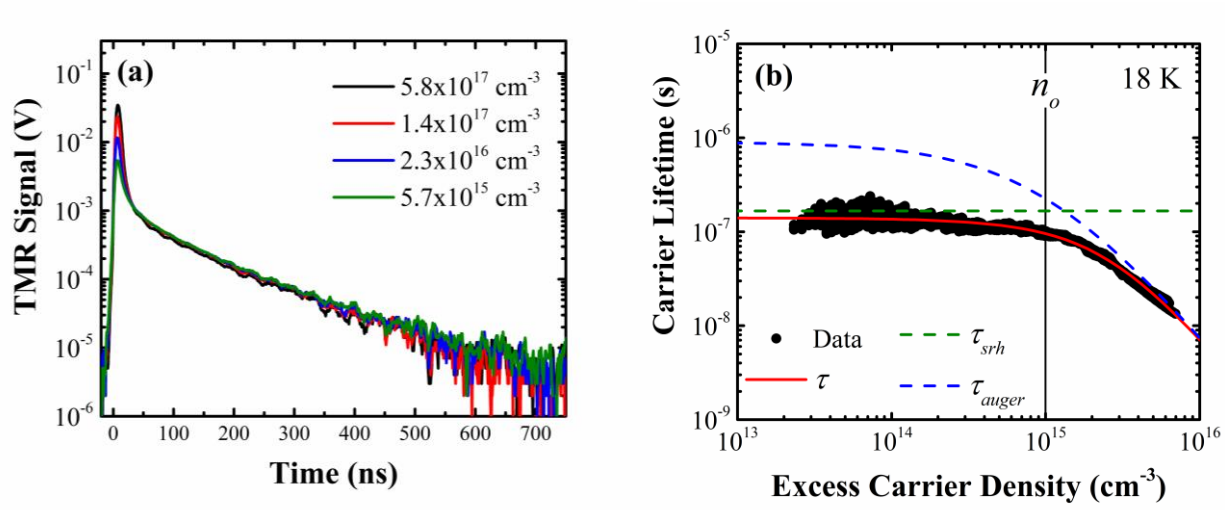

Figure 3. (Colors online) (a) Time-resolved microwave reflectance decays of carrier recombination in the 2 μm thick 47.0 Å InAs/21.5 Å $Ga_{0.75}In_{0.25}Sb$ SL absorber. Data are shown for multiple different initial optically generated carrier densities at a sample temperature of 18 K. (b) Carrier lifetimes as a function of excess carrier density measured at 18 K. The solid red curve is a best fit to the measured data and represents the total lifetime τ. From the fit coefficients, the SRH (τ_{srh}) and Auger (τ_{auger}) lifetime components are also plotted, where $\tau = \left(\tau_{srh}^{-1} + \tau_{auger}^{-1}\right)^{-1}$. Note, the radiative lifetime is not a significant contributor and is not shown. The solid vertical line is the doping level (n_o) extracted from the fit.

The data in Fig. 3b are fit using a function (τ) that includes the dependence that SRH, radiative, and Auger recombination, have on the excess carrier density as,

$$\tau^{-1} = \tau_{srh}^{-1} + \tau_{rad}^{-1} + \tau_{auger}^{-1}, \quad (1)$$

where τ_{srh} is the SRH lifetime, τ_{rad} is the radiative lifetime, and τ_{auger} is the Auger lifetime. The SRH lifetime is,

$$\tau_{srh}^{-1} = \frac{n_o + p_o + \Delta n}{\left(n_o + n_i e^{(E_t - E_i)/k_B T}\right)(\sigma_p v_p N_t)^{-1} + \left(p_o + n_i e^{(E_i - E_t)/k_B T}\right)(\sigma_n v_n N_t)^{-1}}, \quad (2)$$

where σ_n and σ_p are the electron and hole defect capture cross-sections, v_n and v_p are the electron and hole thermal velocities, E_i and E_t are the intrinsic Fermi and SRH defect energies, respectively, N_t is the defect density, k_B is Boltzmann's constant, and T is the temperature. Here, σ_n and σ_p are assumed to be equal and set as the cross section σ. The excess density dependence of the SRH lifetime, when trap saturation is not present, is simply a constant equal to $1/(\sigma_p v_p N_t)$. The radiative lifetime dependence on Δn is,

$$\tau_{rad}^{-1} = B(n_o + \Delta n) = \frac{B_r}{\varphi}(n_o + \Delta n), \quad (3)$$

where B is the radiative coefficient for thick material, B_r is the intrinsic radiative coefficient, φ is the photon recycling factor, and n_o is the SL equilibrium majority carrier electron concentration or doping level. The Auger lifetime is,

$$\tau_{auger}^{-1} = C_n(n_o + \Delta n)^2, \quad (4)$$

where C_n is the Auger coefficient corresponding to the Auger-1 transition [21]. Note, for this analysis n-type material is assumed. The hole-hole Auger coefficient has also been assumed to be negligible in comparison to the electron-electron Auger-1 coefficient [21]. Combining these Equations, the total lifetime is,

$$\tau^{-1} = \tau_{po}^{-1} + B(n_o + \Delta n) + C_n(n_o + \Delta n)^2, \quad (5)$$

with τ_{mc} determined from the low injection limit as,

$$\tau_{mc}^{-1} = \lim_{\Delta n \ll n_o} \tau^{-1} = \frac{1}{\sigma_p v_p N_t} + Bn_o + C_n n_o^2. \quad (6)$$

Since the data in Fig. 3b covers both the high and low injection regimes (i.e. Δn values that are both greater and less than n_o) with good signal-to-noise, Equation 5 can be used to extract the relevant carrier lifetime parameters as well as n_o. The best fit, shown as the red curve in Fig. 3b, provides n_o= 1 x 10^{15} cm^{-3}, τ_{mc} = 140 ± 20 ns, and C_n = 1.1 x 10^{-24} cm^6/s. The radiative component of τ is too small to reliably extract *B*. Figure 3b shows these individual contributions to the total lifetime and at what excess carrier density they limit the minority carrier lifetime. Auger recombination limits τ_{mc} for $\Delta n > n_o$, while SRH recombination limits τ_{mc} for $\Delta n < n_o$. A SRH limited minority carrier lifetime is not surprising as InAs/GaInSb SLs are well known to be SRH limited [23]. The minority carrier lifetime is however markedly long. This τ_{mc} is longer than τ_{mc} reported in binary SLs, which are typically less than 100 ns for MWIR [6, 24, 25] bandgaps and less than 30-35 ns LWIR [6, 8] bandgaps at 77 K. Long wavelength infrared binary SLs have lifetimes less than approximately 50 ns at 20 K [23]. Unfortunately, no reports are available to-date on carrier lifetimes in InAs/GaSb SLs with VLWIR bandgaps, so no direct comparison to the material studied here can be made at this time. Lifetimes in binary and ternary SLs have been previously compared by Youngdale *et al.* at a bandgap of 140 meV though, who found that carrier lifetimes in the ternary SL are generally longer than in the binary SL [26]. We attribute the enhanced minority carrier lifetime determined here to the use of $Ga_{0.75}In_{0.25}Sb$, instead of GaSb, in the SL structure. Using the ternary layer decreases the overall amount of Ga in the ternary SL absorber, decreasing the overall population of Ga-related SRH defects compared to an InAs/GaSb SL. The longer minority carrier lifetime is attributed to an increase in the SRH lifetime compared to the binary SL material system through this reduction in Ga-related recombination centers.

The extracted doping level from the lifetime fit is n_o= 1 x 10^{15} cm^{-3}. From 10 K Hall measurements on similarly grown ternary SL samples, an electron sheet density of 5 x 10^{11} cm^{-2} is typical, corresponding to an electron density of 2.5 x 10^{15} cm^{-3} in the SL characterized here [12]. The n_o extracted from the lifetime analysis correlates very well with this, indicating that the transformation of the TMR decays is without significant error. This result also expresses that carefully calibrated TMR lifetime data, which covers both low and high injection regimes, can be used as an accurate non-destructive probe of the doping level in narrow bandgap IR SL materials.

The Auger coefficient and corresponding low injection level Auger lifetime, which can be determined from Equation 4 assuming $\Delta n << n_o$, are important intrinsic parameters for IR photodetectors. For materials with low defect densities and long SRH lifetimes, the intrinsic Auger processes determine the longest possible minority carrier lifetime and subsequently the best attainable device performance. Since Auger recombination is highly dependent on the SL bandgap and band structure, it is difficult to compare to SL materials of larger bandgaps. In general though, Auger coefficients are proportional to $\propto E_g^{-3/2}\exp(-E_g)$ and increase rapidly with decreasing bandgap energy [9]. Considering the extreme bandgap of this ternary SL, the relatively small measured Auger coefficient is quite encouraging as it suggests the ternary SLs are well suited for IR detection at VLWIR energies.

3.2. Recombination mechanisms

Since identifying the specific recombination mechanisms that are limiting the minority carrier lifetime is critical for future improvement of these materials, we used TMR technique to measure the temperature-dependence of charge carrier recombination in a VLWIR ternary SL absorber that generated a long τ_{mc} at 18 K. Figure 4a shows TMR decays for an initial optically generated carrier density of approximately 7 x 10^{15} cm^{-3} and temperatures ranging from 18 K to 80 K. These data show a general decrease in the long-time decay component from approximately 120 ns at 18 K to 12 ns at 80 K. Note, since the initial carrier density is greater than the equilibrium majority carrier electron concentration (n_o) in this SL, which is approximately 1 x 10^{15} cm^{-3} [16], these decay curves reflect high-injection behavior at short times. This initial rapid decay is due to Auger recombination, which in general scales as the square of the excess carrier density (Δn). The minority carrier lifetime however is measured from the long-time component of the decays, corresponding to excited carrier densities well below the equilibrium electron concentration. The temperature dependence of the equilibrium electron, hole (p_o), and intrinsic (n_i) carrier densities are shown in Fig. 4b, calculated using a 14-band ***k • p*** software and a doping level of n_o = 1 x 10^{15} cm^{-3}.

Proc. of SPIE Vol. 9974 997403-6

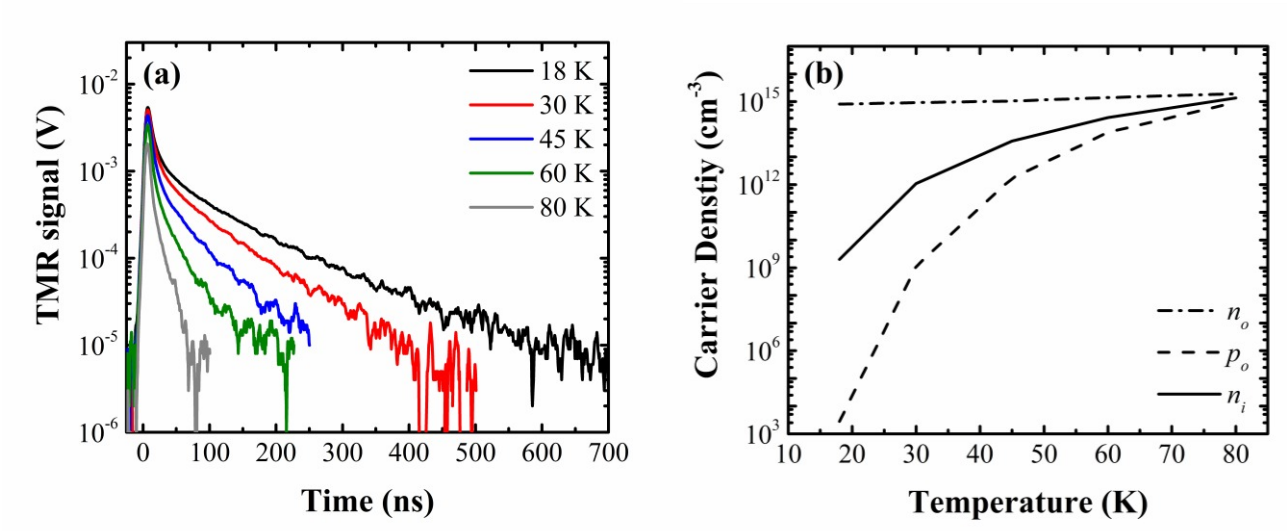

Figure 4. (a) (Color online) Time-resolved microwave reflectance decays as a function of temperature and for an initial optically generated excess carrier density of 7 x 10^{15} cm^{-3}. (b) Temperature dependence of equilibrium electron (n_o), hole (p_o), and intrinsic (n_i) carrier densities for the *n*-type very-long wave infrared InAs/GaInSb superlattice at a doping level of n_o = 1 x 10^{15} cm^{-3}.

These TMR decays are then processed in a manner described previously to accurately extract τ_{mc} [11, 16, 21] and are shown in Fig. 5 as a function of temperature.

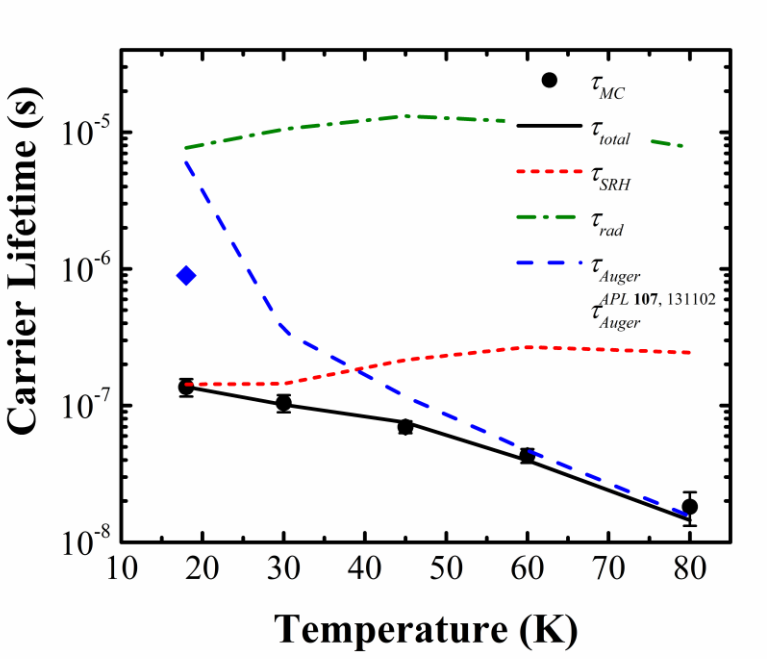

Figure 5. (Color online) Temperature dependence of the minority carrier lifetime (symbols). The blue diamond is the Auger lifetime inferred from injection-dependent carrier lifetime analysis at a temperature of 18 K (Haugan *et al.* [16]). The solid black curve is the best fit to the minority carrier lifetime data, while the rest of the curves are the individual contributions of Shockley-Read-Hall, Auger, and radiative recombination to this total lifetime.

The temperature dependent minority carrier lifetime data is analyzed using the same lifetime equations as the excess density dependent data, except in their low-injection level forms. The full low injection level SRH lifetime is used and can be found by setting $\Delta n << n_0$ in Eq. 2 [21].

For the temperature-analysis, the Beattie, Landsberg, and Blakemore (BLB) form of the Auger lifetime is used, defined as [9, 27].

$$\tau_{auger} = \frac{2n_i^2}{n_0^2+n_o p_o}\tau_{A1}^{(i)}, \tag{7}$$

with the intrinsic Auger-1 lifetime $\tau_{A1}^{(i)}$,

$$\tau_{A1}^{(i)} = 3.8\times10^{-18}\frac{\epsilon_\infty^2(1+\mu)^{1/2}(1+2\mu)}{(m_e/m_o)|F_1F_2|^2}\left(\frac{E_g}{k_BT}\right)^{3/2}\exp\left(\frac{1+2\mu}{1+\mu}\frac{E_g}{k_BT}\right), \tag{8}$$

where ε_∞ is the high frequency dielectric constant, $\mu = m_e/m_h$, m_e is the electron effective mass, m_h is the hole effective mass, m_o is the free electron mass, and $|F_1F_2|$ is the Bloch function overlap integral parameter, which is considered temperature-independent here. However, as will be discussed this is not always valid. Note, the prefactor in Equation 8 has units of seconds. Effective masses from bulk InAs of m_e = 0.026m_o and m_h = 0.46m_o are used here [28]. The radiative lifetime is defined by Equation 3. Prior to fitting the τ_{mc} data the temperature dependence of B_r, E_g, and E_i are calculated with the 14-band ***k*** • ***p*** software using the ternary SL structure as an input. With these and the carrier density data from Fig. 4b, Equations 1-8 are then used to fit the τ_{mc} data with the remaining unknown parameters (E_t, the product of the defect capture cross section and the trap density σN_t, and $|F_1F_2|$) used as fitting parameters. Note, E_t, σNt, and $|F_1F_2|$ are all considered temperature-independent parameters here. The ***k*** • ***p*** modeling indicates that the microscopic radiative lifetime is significantly longer than the measured τ_{mc} data and plays no meaningful part in the carrier recombination dynamics. No information can therefore be learned about photon recycling and φ is set to 1 here. Figure 5 shows the results of this fitting procedure. Auger recombination is found to limit τ_{mc} at temperatures greater than approximately 45 K. Shockley-Read-Hall recombination limits τ_{mc} at very low temperatures below 30 K. The extracted SRH and Auger parameters are listed in Table I.

Table I: Shockley-Read-Hall and Auger recombination parameters determined from temperature-dependent minority carrier lifetime data.

E_t - E_v (meV)	σN_t (1/m)	$\lvert F_1F_2\rvert$
12.6	1.7	0.18

In the intermediate temperature range, both SRH and Auger recombination contribute to the minority carrier recombination dynamics. Interestingly, the Auger lifetime increases dramatically below 30 K. Shown for comparison in Fig. 5 is the Auger lifetime at 18 K determined from intensity-dependent lifetime data [16], which indicates that the Auger lifetime does not increase significantly at lower temperatures. This result is likely a limitation of the assumptions made, when using BLB Auger lifetime equations. At very cold temperatures, charge carriers become restricted to regions of ***k***-space, where Auger matrix elements (or the Auger overlap integrals if considering $|F_1F_2|$) are larger. This effect will correspond to a general leveling off and/or decrease in the Auger lifetime at very cold temperatures [27]. The assumption that $|F_1F_2|$ remain temperature-independent at low temperatures is therefore not valid and in fact must in general increase in magnitude to account for the cooling of carriers to regions of ***k***-space with larger probabilities for an Auger recombination event to occur. What is unknown is how large of an effect this is for the ternary SL investigated here and by how much $|F_1F_2|$ increases as the temperature decreases. In order for the Auger lifetime in Fig. 5 to match the 18 K Auger lifetime datum point, $|F_1F_2|$ would have to increase to approximately 0.55. In totality, the VLWIR ternary SL characterized is of high quality. The measured minority carrier lifetimes are markedly long for material with

such a small bandgap [16]. Additionally, the temperature-dependent analysis suggests that the improvement to be gained by mitigation of the SRH defects would not be substantial at temperatures greater than 45 K, since Auger recombination is found to be the limiting recombination mechanism. The Auger lifetime can be increased through electronic band structure engineering or by reducing the doping level during growth, the latter which isn't always ideal in a photodetector structure. At temperatures below 30 K, the lifetime analysis indicates that approximately an order of magnitude improvement in the minority carrier lifetime could be attained if the SRH recombination defects are mitigated. Considering that diffusion current goes as the inverse of the minority carrier lifetime [21], this improvement in τ_{mc} would correspond to approximately an order of magnitude potential decrease in dark current (with all other values held constant). A discrepancy not mentioned though is that the Auger lifetime found here is significantly shorter than that the theoretical prediction for this ternary SL structure [4]. We attribute this disagreement to variations in the as-grown SL structure compared to the SL structure used in the $\boldsymbol{k \cdot p}$ modeling (e.g. the modeled SL has perfect interfaces, no fluctuations in SL period, etc.). It is well known that Auger recombination rates are highly sensitive to the electronic band structure, layer strains, and bandgap energy, all of which are intimately tied to the type-II SL structure.

4. SUMMARY AND CONCLUSIONS

In conclusion, we have demonstrated long minority carrier lifetimes in infrared materials by using a strain-engineered ternary InAs/GaInSb SL design. A nominal SL structure of 47.0 Å InAs/21.5 Å $Ga_{0.75}In_{0.25}Sb$ that produces an approximately 25 μm response at 10 K generates a long minority carrier lifetime of 140 ± 20 ns, which is markedly long for SL material with such a narrow bandgap. The improved minority carrier lifetime is attributed to mitigation in Ga-related SRH recombination centers by reducing Ga-content in the system. The temperature-dependent data show a general decrease in the long-decay component. Analysis shows that the lifetime decay is dominated by the SRH recombination at temperature below ~30 K, and by the Auger recombination at temperatures above ~45 K. This result indicates that minimal improvement can be made in the minority carrier lifetime at temperatures greater than 45 K without engineering the ternary SL structure to further suppress Auger recombination, which suggests that the improvement to be gained by mitigation of the SRH defects would not be substantial at these temperatures. At temperatures below 30 K, some improvement can be attained by mitigated of the SRH recombination centers. Since the strain-balanced ternary SL design offers a reasonably good absorption coefficient and many epitaxial advantages during growth, this VLWIR SL material system should be considered a competitive candidate for VLWIR photodetector technology.

ACKNOWLEDGMENTS

The work of H. J. Haugan was performed under Air Force contract number FA8650-11-D-5800. The authors thank S. L. Bowers for a technical assistance with the MBE system and X-ray measurements. The lifetime data reported here were conducted at Sandia National Laboratories, and were supported by the U.S. Department of Energy, Office of Science, Basic Energy Science, Materials Science and Engineering Division. Sandia National Laboratories is a multi-program laboratory managed and operated by Sandia Corporation, a wholly owned subsidiary of Lockheed Martin Corporation, for the U. S. Department of Energy's National Nuclear Security Administration under contract DE-AC04-94AL85000. The authors thank Prof. Michael Flatté at the University of Iowa for use of his $\boldsymbol{k \cdot p}$ software.

REFERENCES

[1] D. L. Smith and C. Mailhiot, "Proposal for strained type II superlattice infrared detectors", J. Appl. Phys. **62**, 2545 (1987).
[2] H. Kroemer, "The 6.1 Å (InAs, GaSb, AlSb) and its heterostructures: a selective review", Physica E **20**, 196 (2004).
[3] J. L. Johnson, L. A. Samoska, A. C. Gossard, J. L. Merz, M. D. Jack, G. R. Chapman, B. A. Baumgratz, K. Kosai, and S. M. Johnson, "Electrical and optical properties of infrared photodiodes using the $InAs/Ga_{1-x}In_xSb$ superlattice in heterojunctions with GaSb", J. Appl. Phys. **80**, 1116 (1996).
[4] C. H. Grein, W. H. Lau, T. L. Harbert, and M. E. Flatté, "Modeling of very long infrared wavelength InAs/GaInSb strained layer superlattice detectors", Proc. SPIE. **4795**, 39 (2002).
[5] M. Razeghi, Y. Wei, A. Gin, G. J. Brown, and D. Johnstone, "Type-II InAs/GaSb superlattices and detectors with λ_c > 18 μm", Proc. SPIE **4650**, 111 (2002).

[6] D. Donetsky, G. Blenky, S. Svensson, and S. Suchalkin, "Minority carrier lifetime in type-2 InAs-GaSb strained-layer superlattices and bulk HgCdTe materials", Appl. Phys. Lett. **97**, 052108 (2010).
[7] H. J. Haugan, G. J. Brown, F. Szmulowicz, S. Elhamri, B. V. Olson, T. F. Boggess, and L. Grazulis, "The role of InAs thickness on the material properties of InAs/GaSb superlattices", Proc. SPIE. **8154**, 81540J (2011).
[8] H. J. Haugan, G. J. Brown, S. Elhamri, S. Pacley, B. V. Olson, and T. F. Boggess, "Post growth annealing study on long wavelength infrared InAs/GaSb superlattices", J. Appl. Phys. **111**, 053113 (2012).
[9] J. Blakemore, *Semiconductor Statistics* (Dover Publications Inc., New York, 1962).
[10] Y. Aytac, B. V. Olson, J. K. Kim, E. A. Shaner, S. D. Hawkins, J. F. Klem, M. E. Flatté, and T. F. Boggess, "Effect of layer thickness and alloy composition on carrier lifetimes in mid-wave infrared InAs/InAsSb superlattices", Appl. Phys. Lett. **105**, 022107 (2014).
[11] A. M. Hoang, G. Chen, R. Chevallier, A. Haddadi, and M. Razeghi, "High performance photodiodes based on InAs/InAsSb type-II superlattices for very long wavelength infrared detection", Appl. Phys. Lett. **104**, 251105 (2014).
[12] H. J. Haugan, G. J. Brown, S. Elhamri, W. C. Mitchel, K. Mahalingam, M. Kim, G. T. Noe, N. E. Ogden, and J. Kono, "Impact of growth temperature on InAs/GaInSb strained layer superlattices for very long wavelength infrared detection", Appl. Phys. Lett. **101,** 171105 (2012).
[13] H. J. Haugan, G. J. Brown, K. Mahalingam, L. Grazulis, G. T. Noe, N. E. Ogden, and J. Kono, "Optimum growth window for InAs/GaInSb superlattice materials tailored for very long wavelength infrared detection", J. Vac. Sci. Technol. B **32**, 2C109 (2014).
[14] H. J. Haugan, G. J. Brown, K. Mahalingam, and L. Grazulis, "Growth optimization studies to develop InAs/GaInSb superlattice materials for very long wavelength infrared detection", Infrared Phys. Technol. **70**, 99 (2015).
[15] H. J. Haugan, G. J. Brown, S. Elhamri, and L. Grazulis, "Control of anion incorporation in the molecular beam epitaxy of ternary antimonide superlattices for very long wavelength infrared detection", J. Cryst. Growth **425**, 25 (2015).
[16] H. J. Haugan, G. J. Brown, B. V. Olson, E. A. Kadlec, J. K. Kim, and E. A. Shaner, "Demonstration of long minority carrier lifetimes in very narrow bandgap ternary InAs/GaInSb superlattices", Appl. Phys. Lett. **107**, 131102 (2015).
[17] H. J. Haugan, G. J. Brown, B. V. Olson, E. A. Kadlec, J. K. Kim, and E. A. Shaner, "Minority carrier lifetimes in very long-wave infrared InAs/GaInSb superlattices", J. Vac. Sci. Technol. B **34**, 02L104 (2016).
[18] H. J. Haugan, L. Grazulis, G. J. Brown, K. Mahalingam, and D. H. Tomich, "Exploring optimum growth for high quality InAs/GaSb type-II superlattices", J. Cryst. Growth **261**, 471 (2004).
[19] H. J. Haugan, G. J. Brown, S. D. Pacley, L. Grazulis, and S. T. Fenstermaker, "Study of strain balance in long wavelength infrared InAs/GaSb superlattice materials", M. Kim, K. Mahalingam**,** S. Elhamri, W. C. Mitchel, and L. Grazulis**,** Proc. SPIE. **7804**, 780806 (2010).
[20] H. J. Haugan, G. J. Brown, and L. Grazulis, "Effect of interfacial formation on the properties of very long wavelength infrared InAs/GaSb superlattices", J. Vac. Sci. Technol. B **29**, 03C101 (2011).
[21] B. V. Olson, E. A. Kadlec, J. K. Kim, J. F. Klem, S. D. Hawkins, E. A. Shaner, and M. E. Flatté, "Intensity- and temperature-dependent carrier recombination in InAs/$InAs_{1-x}Sb_x$ type-II superlattices", Phys. Rev. App. **3**, 044010 (2015).
[22] B. V. Olson, C. H. Grein, J. K. Kim, E. A. Kadlec, J. F. Klem, S. D. Hawkins, and E. A. Shaner, "Auger recombination in long-wave infrared InAs/$InAs_{1-x}Sb_x$ type-II superlattices", Appl. Phys. Lett. **107**, 261104 (2015).
[23] B. C. Connelly, G. D. Metcalfe, H. Shen, and M. Wrabeck, "Direct minority carrier lifetime measurements and recombination mechanisms in long-wave infrared type II superlattices using time-resolved photoluminescence", Appl. Phys. Lett. **97**, 251117 (2010).
[24] S. P. Svensson, D. Donetsky, D. Wang, H. Hier, F. J. Crowne, and G. Belenky, "Growth of type II strained layer superlattice, bulk InAs and GaSb materials for minority lifetime characterization", J. Cryst. Growth **334**, 103 (2011).
[25] L. M. Murray, K. S. Lokovic, B. V. Olson, A. Yildirim, T. F. Boggess, and J. P. Prineas, "Effects of growth rate variations on carrier lifetime and interface structure in InAs/GaSb superlattices", J. Crystal Growth **386**, 194 (2014).
[26] E. R. Youngdale, J. R. Meyer, C. A. Hoffman, F. J. Bartoli, R. H. Miles, and D. H. Chow, "Recombination lifetime in InAs-$Ga_{1-x}In_xSb$ superlattices", J. Vac. Sci. Technol. B **12**, 1129 (1994).
[27] C. H. Grein, P. M. Young, M. E. Flatté, and H. Ehrenreich, "Long wavelength InAs/InGaSb infrared detectors: Optimization of carrier lifetimes", J. Appl. Phys. **78**, 7143 (1995).
[28] B. V. Olson, E. A. Shaner, J. K. Kim, J. F. Klem, S. D. Hawkins, M. E. Flatté, and T. F. Boggess, "Identification of dominant recombination mechanisms in narrow-bandgap InAs/InAsSb type-II superlattices and InAsSb alloys", Appl. Phys. Lett. **103**, 052106 (2013).